

NEAT: a space born astrometric mission for the detection and characterization of nearby habitable planetary systems

Fabien Malbet^a, Renaud Goullioud^b, Pierre-Olivier Lagage^c, Alain Léger^d, Mike Shao^b,
Antoine Crouzier^a, and the NEAT consortium^e

^aUJF-Grenoble 1 / CNRS-INSU, Institut de Planétologie et d'Astrophysique de Grenoble (IPAG), UMR 5274, Grenoble, France

^bJet Propulsion Laboratory (JPL), California Institute of Technology, Pasadena, USA

^cLaboratoire AIM, CEA-IRFU / CNRS-INSU / Université Paris Diderot, CEA Saclay, Gif-sur-Yvette Cedex, France

^dUniversité Paris Sud / CNRS-INSU, Institut d'Astrophysique Spatiale (IAS) UMR 8617, Orsay, France

^eFull list of NEAT proposal members at <http://neat.obs.ujf-grenoble.fr>

ABSTRACT

The NEAT (Nearby Earth Astrometric Telescope) mission is a proposal submitted to ESA for its 2010 call for M-size mission within the Cosmic Vision 2015-2025 plan. The main scientific goal of the NEAT mission is to detect and characterize planetary systems in an exhaustive way down to 1 Earth mass in the habitable zone and further away, around nearby stars for F, G, and K spectral types. This survey would provide the actual planetary masses, the full characterization of the orbits including their inclination, for all the components of the planetary system down to that mass limit. NEAT will continue the work performed by Hipparcos and Gaia by reaching a precision that is improved by two orders of magnitude on pointed targets.

Keywords: Space mission, astrometry, exoplanets

1. INTRODUCTION

Exoplanet research has grown explosively in the past decade, supported by improvements in observational techniques that have led to increasingly sensitive detection and characterization. Among many results, we have learned that planets are common, but their physical and orbital properties are much more diverse than originally thought.

A lasting challenge is the detection and characterization of planetary systems consisting in a mixed cortege of telluric and giant planets, with a special regard to telluric planets orbiting in the habitable zone (HZ) of Sun-like stars. The accomplishment of this goal requires the development of a new generation of facilities, due to the intrinsic difficulty of detecting Earth-like planets with existing instruments. The proposed NEAT mission has been designed to enter a new phase in exoplanetary science by delivering an enhanced capability of detecting small planets in the Habitable Zone

In Sect. 2, we present the science objectives of NEAT, we describe the principle of the differential astrometry technique and we give a list of potential targets. In Sect. 3, after listing the technical challenges, we present the instrumental concept. We explain how to reach the performance and we give a summarized description of the payload, the mission and the spacecraft. In Sect. 4, we discuss both astrophysical and technical issues. Recommendations by the community summarized in Sect. 5 is an incentive to pursue the development of this mission in the future.

Further author information: (Send correspondence to Fabien.Malbet@obs.ujf-grenoble.fr)

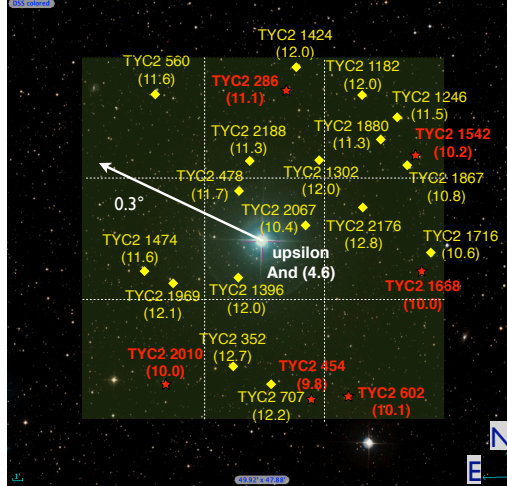


Figure 1. 0.3° stellar field around upsilon Andromedae, a proposed NEAT target. There are six possible reference stars in this field marked in red (five $V < 11$ stars and a $V = 11.1$ one).

2. SCIENCE OBJECTIVES

2.1 Main science questions

The prime goal of NEAT is to detect and characterize planetary systems orbiting bright stars in the solar neighborhood that have a planetary architecture like that of our Solar System or an alternative planetary system made of Earth mass planets. It will allow the detection around nearby stars of planets equivalent to Venus, Earth, (Mars), Jupiter, and Saturn, with orbits possibly similar to those in our Solar System. It will permit to detect and characterize the orbits and the masses of many alternate configurations, e.g. where the asteroid belt is occupied by another Earth mass planet and no Jupiter. The NEAT mission will answer the following questions:

- What are the dynamical interactions between giant and telluric planets in a large variety of systems?
- What are the detailed processes involved in planet formation as revealed by their present configuration?
- What are the distributions of architectures of planetary systems in our neighborhood up to ≈ 15 pc?
- What are the masses, and orbital parameters, of telluric planets that are candidates for future direct detection and spectroscopic characterization missions?

Special emphasis will be put on planets in the *Habitable Zone* because this is a region of prime interest for astrobiology. Indeed orbital parameters obtained with NEAT will allow spectroscopic follow-up observations to be scheduled precisely when the configuration is the most favorable.

2.2 High-precision differential astrometry

The principle of NEAT is to measure accurately the offset angles between a target and 6-8 distant reference stars with the aim of differentially detecting the reflex motion of the target star due to the presence of its planets. An example of a field that will be observed is shown in Fig. 1 and a simulation of what will be measured is displayed in Fig. 2.

The output of the analysis is a *comprehensive* determination of the mass, orbit, and ephemeris of the different planets of the *multiplanetary system* (namely the 7 parameters M_P , P , T , e , i , ω , Ω), down to a given limit depending on the star characteristics, e.g. 0.5, 1 or $5 M_\oplus$. The astrometric amplitude, A , of a M_* mass star due to the reflex motion in presence of a M_P mass planet orbiting around with a semi-major axis a at a distance D from the Sun is

$$A = 0.3 \left(\frac{M_P}{1 M_\oplus} \right) \left(\frac{a}{1 \text{ AU}} \right) \left(\frac{M_*}{1 M_\odot} \right)^{-1} \left(\frac{D}{10 \text{ pc}} \right)^{-1} \mu\text{as}. \quad (1)$$

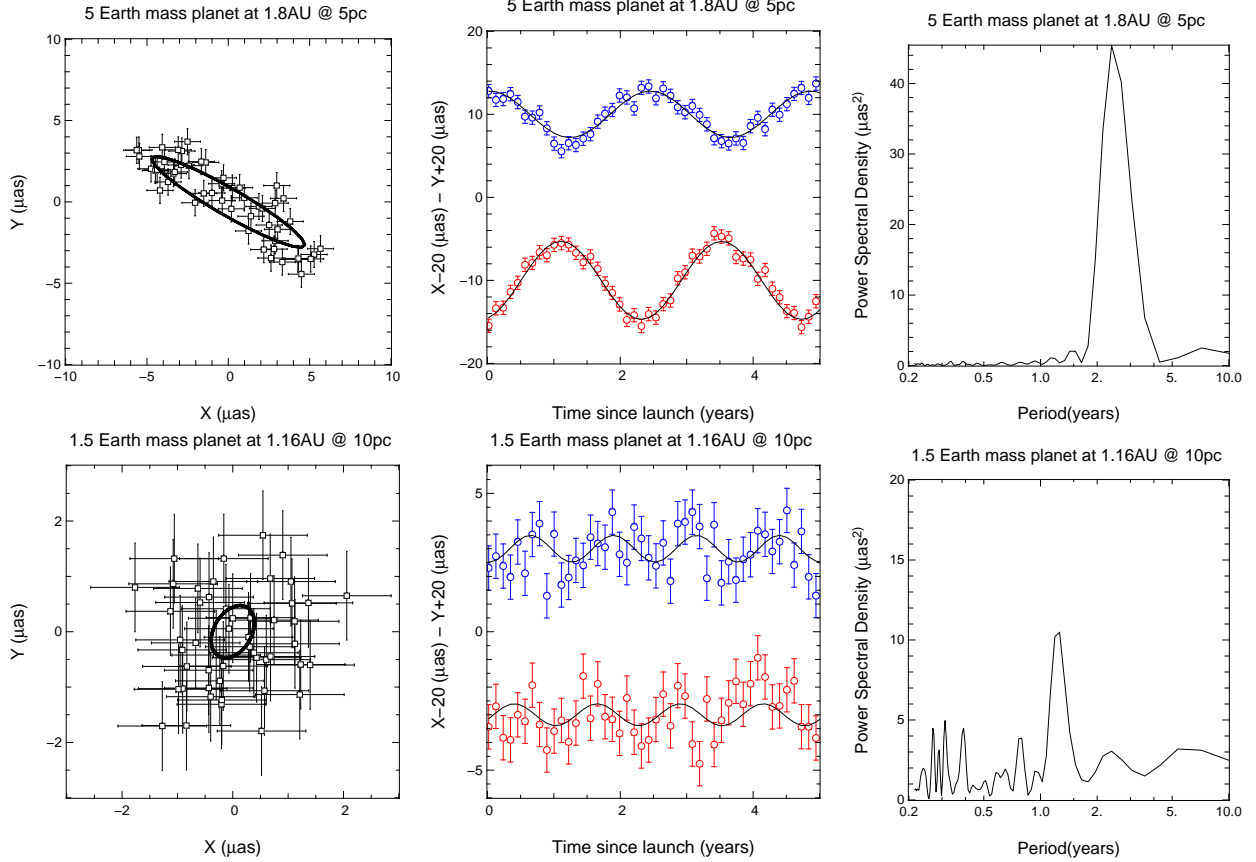


Figure 2. Simulation of astrometric detection of two type of planets with 50 NEAT measurements (RA and DEC) over 5 yrs. Top row parameters corresponds to an easy detection: $M_P = 5 M_\oplus$, $a = 1.8 AU$, $M_* = 1 M_\odot$, $D = 5 pc$. Bottom row parameters corresponds to a more challenging detection: $M_P = 1.5 M_\oplus$, $a = 1.16 AU$, $M_* = 1 M_\odot$, $D = 10 pc$. Left panels: sky plot showing the astrometric orbit (solid curve) and the NEAT measurements with error bars; middle panels: same data but shown as time series of the RA and DEC astrometric signal (an offset has been put to separate them); right panels: joint Lomb-Scargle periodogram for right ascensions and declinations simultaneously. All measurements corresponds to 1 h visits with a $0.8 \mu as$ precision. This precision can be improved or degraded by a longer or a shorter visit time.

To detect such a planet, one needs to reach a precision $\sigma = A/SNR$ with a typical signal-to-noise ratio $SNR = 6$. If σ_0 is the precision that NEAT can reach in one single observation that lasts t_0 (e.g. $\sigma_0 = 0.8 \mu as$ in $t_0 = 1 h$), when observing the same source N_{visits} times during T_{visit} each visit requires

$$T_{visit} = t_0 \left(\frac{A}{SNR \sigma_0} \right)^{-2} (2N_{visits} - m)^{1/2} \quad (2)$$

for a given N_{visits} , and with $m = 5 + 7p$ parameters where p is the number of planets in the system since there are 5 parameters characterizing the star astrometric motion and 7 parameters for each orbit. $N_{visits} \approx 50$ is sufficient to solve for the parameters of 3 to 5 planets per system, for a 5-yr duration of the mission.

2.3 Targets

The spatial repartition of stars within 20 pc is shown in Fig. 3. As for the date of May 2012, only 5% are known to host exoplanets because of stellar activity problems and brightness issues. Most of the more than 700 exoplanets known in May 2012 are located further away than the first 20 pc.

A possible target list is shown in Table 1 where we consider the list of the nearest F, G, K stars deduced from the Hipparcos 2007 catalogue (new data reduction¹), disregarding spectroscopic binaries, and stars with an

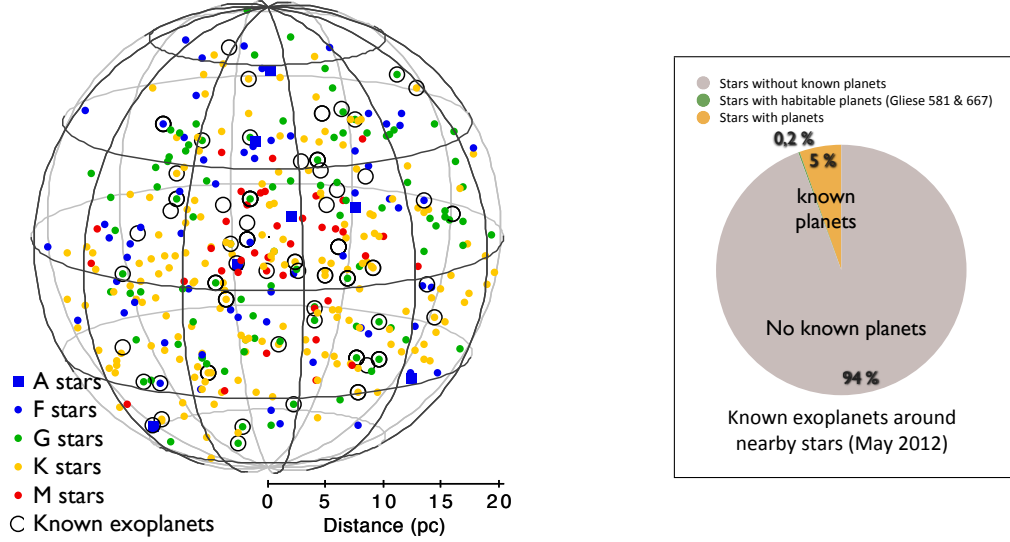


Figure 3. Left: representation of the NEAT targets in the 3D sphere of our neighborhood (D up to ≈ 20 pc). Right: number of these stars with known exoplanets. Only 5% of these stars are known to host exoplanets.

Table 1. Partial list of possible targets. Stars are ranked by decreasing astrometric signal for a planet in its habitable zone (HZ). This signal $A(\mu\text{as})$ is calculated for 0.5, 1 and 5 M_{\oplus} planets around the 5, 70 and 200 first stars, respectively, assuming that the planet is located at the inner boundary of the HZ that secures its detection whenever the planet is in this zone. The corresponding integration time (t_{visit} in h) and cumulated times (t_{tot} in h) are calculated for a detection with an equivalent SNR = 6.

Rank	Star_ident.	Name	Vmag	SpType	D (pc)	LogR ^{HK}	HZ _{in} (AU)	t_{tot} (h)	$A(\mu\text{as})$ t_{visit} (h)						
									$M_{\text{planet}} = 0,5 M_{\oplus}$	$M_{\text{planet}} = 1 M_{\oplus}$	$M_{\text{planet}} = 5 M_{\oplus}$	$M_{\text{planet}} = 0,5 M_{\oplus}$	$M_{\text{planet}} = 1 M_{\oplus}$	$M_{\text{planet}} = 5 M_{\oplus}$	$M_{\text{planet}} = 0,5 M_{\oplus}$
1	HIP16537	eps Eri	3,72	K2V	3,2	-4,620	0,57	139	0,35	2,5					
2	HIP8102	LHS 146	3,49	G8V	3,7	-4,958	0,58	337	0,29	3,7					
(...)								-	-	-					
4	HIP104214	61 Cyg A	5,20	K5V	3,5	-4,764	0,34	804	0,25	4,8					
5	HIP19849	40 Eri	4,43	K1V	5,0	-5,380	0,62	1 094	0,24	5,6					
7	HIP99240	del Pav	3,55	G5IV	6,1	-5,000	0,96	1 265			0,45	1,5			
8	HIP96100	sig Dra	4,67	K0V	5,8	-4,832	0,63	1 357			0,44	1,6			
(...)								-			-	-			
69	HIP64797	LTT 13852	6,49	K2V	11,1	-4,630	0,56	16 957			0,20	7,5			
70	HIP23835	LHS 1736	4,91	G4V	15,4	-5,127	1,26	17 349			0,20	7,6			
71	HIP47592	LTT 3558	4,93	G0V	15,0	-4,862	1,18	17 377					1,00	0,31	
72	HIP26779	V538 Aur	6,21	K1V	12,3	-4,550	0,68	17 405					1,00	0,31	
(...)								-					-	-	
199	HIP79537	LHS 413	7,53	K0V	12,9	-5,205	0,41	22 013					0,70	0,64	
200	HIP18859	HD 25457	5,38	F5V	18,8	-4,600	1,02	22 058					0,69	0,65	

activity level 5 times greater than that of the Sun because of their astrometric noise (only 4% of the sample²) and for which we compute the astrometric signal for a planet with given mass in the HZ of the stars.³ Conservatively, we select the inner part of the HZ in order to be able to detect the planet whatever is its location in the HZ. The required number of visits and cumulative time to observe this list of target stars is summarized in Table 2. The list corresponds to an exhaustive search for 1 Earth mass planets (resp. 5 Earth mass planets) around K stars up to 6 pc (resp. 12 pc), G stars up to 10 pc (resp. 17 pc), and F stars up to 14 pc (resp. 19 pc) in the whole HZ of the star, excluding spectroscopic binaries and very active stars.

60% of the NEAT targets (118) are brighter than $V = 6$ and therefore will not be investigated by Gaia because of its bright limit. So, even if some of those sources do not harbor Earth-like planets, NEAT will be contributing to the improvement of our knowledge about the neighborhood of our Solar System. In that respect, NEAT observations will not only be complementary to Gaia's ones, but NEAT data will also form a base to improve Gaia results.

Table 2. Left: summary of the main program capabilities and required resources. Right: Time and allocated maneuvers for the different programs: (1) the Gaia Mission and its Exoplanet Science Potential; (2) NEAT follow-up program of Gaia detected planetary systems; (3) observations of young stars; and (4) characterizing planetary systems around some of the closest A and M stars.

Number of stars	Mass threshold (M_{\oplus})	Cumulated time (h)	Number of visits	Program	Time (h)	Maneuvers
5	0.5	1,100	500	Transfert + com.	3,650	
70	1	15,600	3,500	Main	22,100	10,000
200	5	6,400	6,000	Add. 1-3	5,500	2,000
				Add. 4	2,750	1,000
				total margins	9,800 (22%)	7,000
Total		22,100	10,000	Total	43,800 h (5 yrs)	20,000

In addition to the survey for the NEAT main science program, we propose that 30% of NEAT time is allocated to study some objects of interest (planets around A stars and M dwarfs, young stars, multiple systems,... discovered by Gaia and others). The global required amount of time and number of maneuvers is listed in the right Table 2.

3. NEAT CONCEPT

Our goal is to detect the signal corresponding to the reflex motion of a Sun-like star at 10 pc due to an Earth-mass planet in its HZ, with an equivalent final SNR of 6. That astrometric signal is $0.3 \mu\text{as}$. The required end-of-mission noise floor is $0.05 \mu\text{as}$, over 100 times lower than Gaia’s best precision which is $7 \mu\text{as}$.

3.1 Technical challenges

Achieving sub-micro-arcsecond astrometric precision, e.g. $0.8 \mu\text{as}$, in 1 hour and a noise floor under $0.05 \mu\text{as}$ with a telescope of diameter D requires mastering all effects that could impact the determination of the position of the point spread function. The typical diffraction limited size of an unresolved star is about $1.2\lambda/D$, which corresponds to 0.16 arcseconds for a 1-m telescope operating in the visible spectral region. Even though differential astrometry of stars within the same field of view softens somewhat the requirement, this level of accuracy can only be obtained in an atmosphere-free space environment.

Sub-micro-arcsecond level astrometry requires solutions to four challenges:

- **Photon noise.** Most target stars are bright ($R \leq 6$ mag), but the associated reference stars are faint, therefore their brightness dominates the photon noise. Using the mean stellar density in the sky, one finds that a field of view (FOV) as large as diam 0.6° is needed to get several (6 to 8) of $R \leq 11$ mag references (see e.g. Fig 1).
- **Beam walk.** A classical three mirror anastigmat (TMA) telescope can manage a 0.6° diffraction limited FOV. However the light coming from different stars, and therefore from different directions, will hit the secondary and tertiary mirrors on very different physical parts of the mirrors. The mirror defects will therefore produce different and prohibitive astrometric errors between the images of the stars. Using a single mirror telescope solves this problem. To obtain sufficiently high angular resolution, a long focal length for this mirror is needed, with no intermediate mirrors, a relatively unusual solution in modern optical astronomy.
- **Stability of the focal plane.** Proper Nyquist sampling with typical detector pixels of the order of $10 \mu\text{m}$ requires a focal plane at a focal length of 40 m. Such a focal plane covering a FOV of 0.6° diameter would yield a costly detector mosaic with $40,000 \times 40,000 \approx 10^9$ pixels. Sub-microarcsec astrometry over a 0.6° -diameter FOV requires the geometry of the focal plane to be stable to $\approx 1 : 2 \times 10^{-10}$. Instead of building a gigapixel focal plane with unprecedented stability we plan to use 9 small 512×512 CCDs (right part of Fig. 4) and a laser metrology system to measure the position of every pixel to the required precision, once every 10 to 30 s. We do not rely on their positioning and stability, but we measure it accurately and frequently with a laser metrology based on dynamic interference fringes.

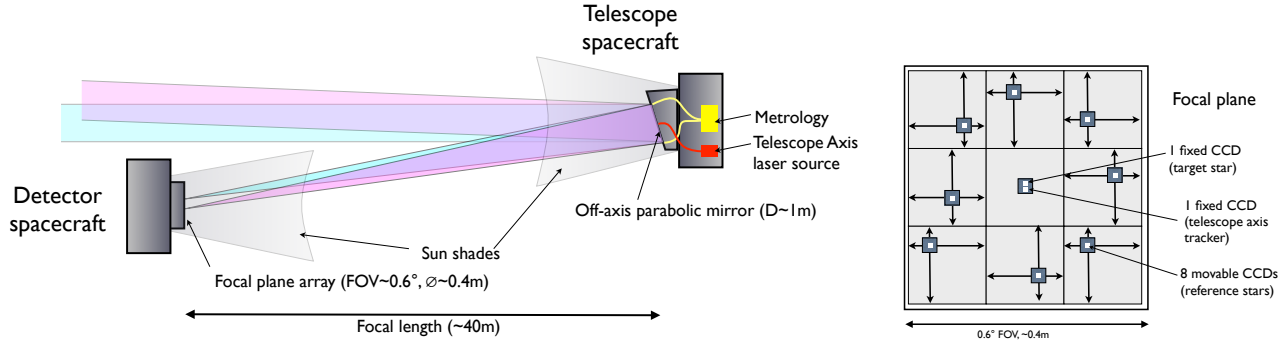


Figure 4. Proposed concept for a very high precision astrometry mission. Left: the instrument consists in two separated modules, the first one carrying the primary mirror (upper right) and the second one the detector plane (bottom left). Right: schematic layout of the focal plane. The field of view is divided in 3×3 sub-fields. Outer subfields have visible arrays which can be moved in X and Y directions to image the reference stars. The central field has two fixed arrays, one for the target star and one for the telescope axis tracker.

- **Quantum efficiency (QE) variations.** At the level of accuracy required by this mission, the measurement of the inter- and intra-pixel QE variations is mandatory. Thanks to the dynamic fringes of the calibration system, each pixel response can be characterized^{4,5} with six parameters such that the systematic errors are kept below 10^{-6} .

3.2 Instrumental concept

The proposed mission is based on a concept that results from the experience gained in working with many astrometry concepts (SIM, SIM-Lite, corono-astrometry⁶). The concept is sketched in left part of Fig. 4 and consists of a primary mirror —an off-axis parabolic 1-m mirror— a focal plane 40 m away, and metrology calibration sources. The large distance between the primary optical surface and the focal plane can be implemented as two spacecraft flying in formation, or a long deployed boom. The focal plane with the detectors having a field of view of 0.6° is shown in the right part Fig. 4. It has a geometrical extent of $0.4\text{m} \times 0.4\text{m}$. The focal plane is composed of eight 512×512 visible CCDs located each one on an XY translation stage while the central two CCDs are fixed in position. The CCD pixels are $10\mu\text{m}$ in size.

The principle of the measurement is to point the spacecraft so that the target star, which is usually brighter ($R \leq 6$) than the reference stars ($R \leq 11$), is located on the axis of the telescope and at the center of the central CCD. Then the 8 other CCDs are moved to center each of the reference stars on one of them. To measure the distance between the stars, we use a metrology calibration system that is launched from the telescope spacecraft and that feeds several optical fibers (4 or more) located at the edge of the mirror. The fibers illuminate the focal plane and form Young's fringes detected simultaneously by all CCDs (Fig. 5). The fringes have their optical wavelengths modulated by acoustic optical modulators that are accurately shifted by 10 Hz, from one fiber to the other so that fringes move over the CCDs^{5,7} or by phase modulator.⁸ These fringes allow us to solve for the XYZ position of each CCD. An additional benefit from the dynamic fringes on the CCDs is to measure the QE of the pixels (inter- and intra-pixel dependence). The CCDs are read at 50 Hz providing many frames that will yield high accuracy.

With the proposed concept, it is possible to achieve all the main technical requirements:

- **Focal plane stability.** Instead of maintaining a focal plane geometry stable at the 0.1 nm level for a 5-yr duration, which is impossible, we get advantage of a metrology for every pixel at the sub-nanometer level which is used every minute.
- **Reference frame.** By measuring the fringes at the sub-nanometer level and by using the information from all the pixels of each CCD, it is possible to solve for the position of all reference stars compared to the central target with an accuracy of $0.8 \mu\text{as}/\sqrt{h}$. The field of view of 0.6° allows us to have 6 to 8 reference stars brighter than $V = 11$ in most fields.

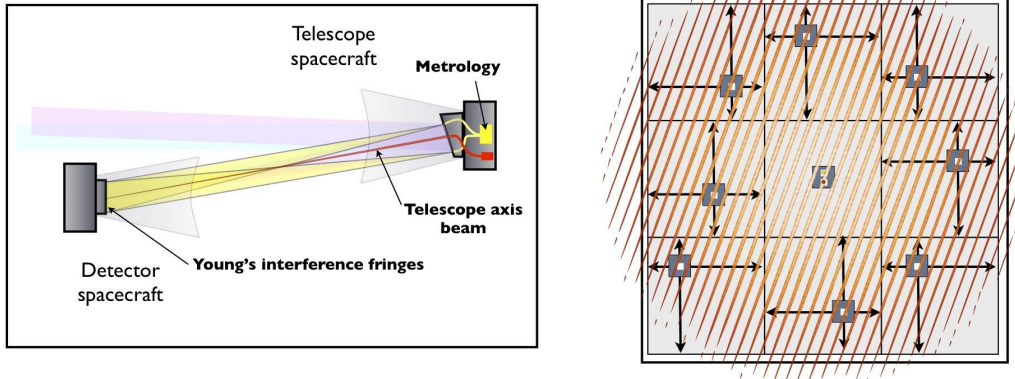


Figure 5. Principle of the metrology and the axis tracker. Left panel: the metrology laser light (in yellow) is launched from fibers located at the edge of the mirrors. Right panel: the laser beams interfere over the detector plane. Only the fringes corresponding to a pair of fibers are represented on this figure and they are not to scale, since the fringe spacing is equal to the PSF width. The axis tracker (sketched in red on the left panel) is a laser beam launched in the center of the mirror that is monitored in the lower central CCD.

- **Photon noise.** The field of 0.6° provides about 6 to 8 stars of magnitude brighter than $R = 11$. The number of photons received by one 11-mag star on the system is $\approx 4.1 \times 10^9$ ph/hr. Since the FWHM of diffraction-limited stars is $1.2\lambda/D = 0.16$ arcsecond, the photon noise limit in 1 h of integration due to a set of 6 reference stars is $(\lambda/2D)/\sqrt{6N} \approx 0.5 \mu\text{as}$. With more than 50×2 measurements of a few hours spread over 5 yrs, the equivalent precision is $0.05 \mu\text{as}$ in RA and Dec, corresponding to the detection of the $0.30 \mu\text{as}$ signal with a $\text{SNR} \approx 6$.
- **Large-scale calibration.** The detector plane does not have to be fully covered by pixels, since the positions of the reference stars are known from available catalogues (10-20 mas for Tycho 2, and about tens of μas for Gaia). For the target stars ($R \leq 6$), we use the Hipparcos catalog (few mas accuracy). This corresponds to $< 1/10^{\text{th}}$ of the PSF or the fringe width. The number of fringes between the target star and the reference stars is then known, only the positions of the star centroids relative to the interferometric fringes have to be measured accurately.

The use of 10 small CCDs drastically reduces the cost of what would otherwise be a giga-pixel focal plane and also helps to control systematics. With such a concept, the mission performance would be similar to, and even more favorable for exoplanets, than what was proposed for SIM-Lite with 5 years of operation, but at the price of giving up all-sky astrometry and the corresponding science objectives.

3.3 Performance assessment and error budget

NEAT will not be capable of measuring the absolute separation between the target and the set of reference stars to $0.8 \mu\text{as}$. NEAT objectives is to measure the change in the *relative* position of those stars between successive observations spread over the mission life, with an error of $0.8 \mu\text{as}$ for each one hour visit. Achieving our target precision relies on not only the metrology stability, but also on the precise knowledge of the positions of the multiple reference stars used since the expected motions of the references cannot be considered as fixed (see discussion in Sect. 4.1). Our comprehensive error budget takes into account all sources of error, including instrumental effects, photon noise and astrophysical errors in the reference star positions.

The six major errors terms are captured in the simplified version of the error budget shown in Fig. 6. The biggest term is the brightness dependent error for the set of reference stars. Static figure errors of the primary mirror will produce centroid offsets that are mostly common-mode across the entire field of view. Differential centroid offsets are significantly smaller than the field-dependent coma and are in fact negligible. Similarly, changes in the primary mirror surface error, e.g. due to thermal dilatation, meteorite impacts,... produce mostly common-mode centroid shifts and negligible differential centroid offsets. On the other hand, displacement and

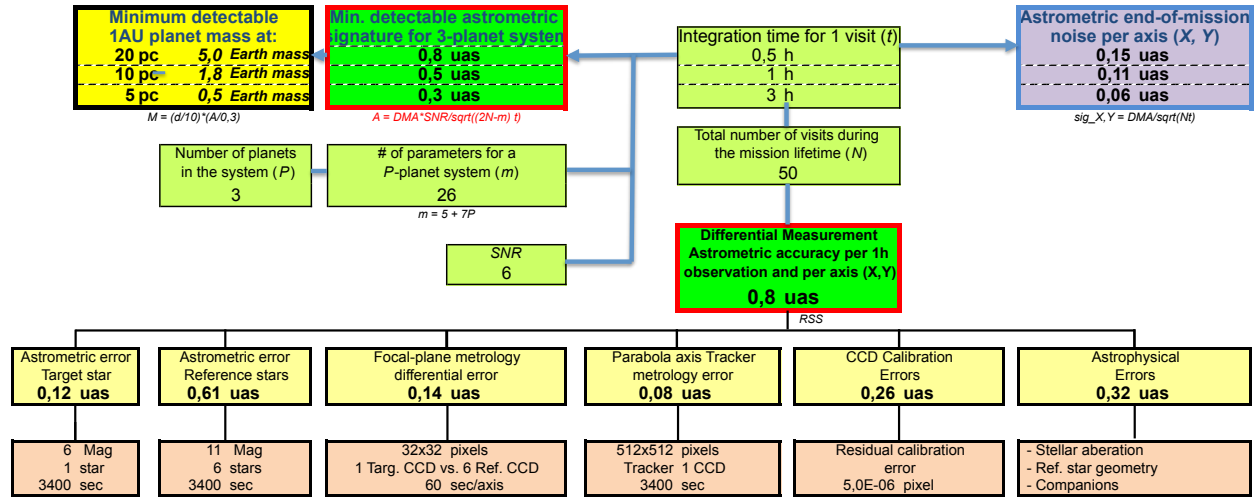


Figure 6. Top-level error budget for NEAT that shows the major contributor to the overall budget. It also shows how the $0.8 \mu\text{as}/\sqrt{h}$ accuracy enables the detection of $0.3 \mu\text{as}$ (resp. $0.5 \mu\text{as}$ and $0.8 \mu\text{as}$) signatures with a signal to noise of 6 after 50 visits of 3 h (resp. 1 h and 0.5 h) of observation that allows a $0.5 M_{\oplus}$ planet at 5 pc to be detected (resp. $1.8 M_{\oplus}$ at 10 pc and $5 M_{\oplus}$ at 20 pc).

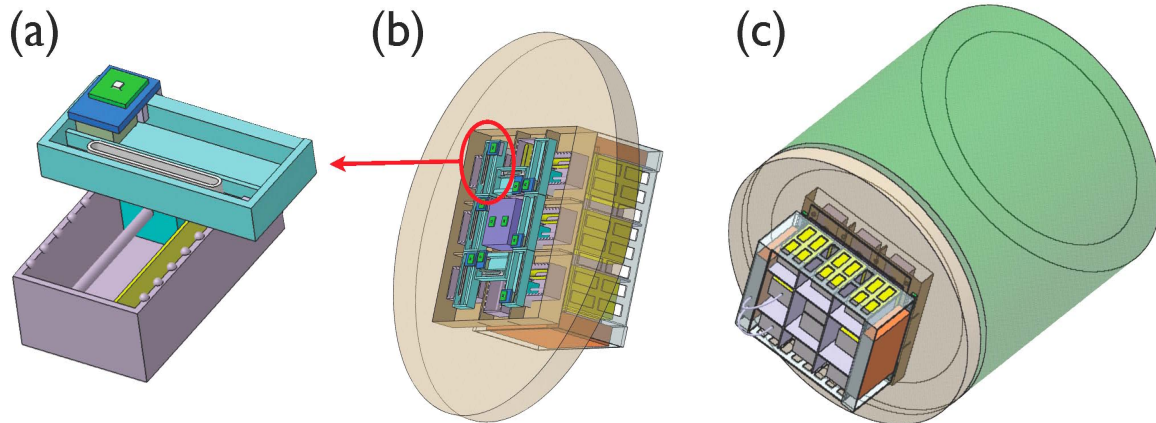


Figure 7. Views of the focal plane assembly. (a) Magnified view of one of the 8 XY translation stages of the focal plane. In yellow, the 512×512 CCD and its support. In blue and green the two translation stages. (b) The front part of the focal plane with its 8 movable CCDs and two fixed CCDs at the center. (c) The electronics racks.

changes in the shape of the PSF would couple with the CCD response if the CCD response is not properly calibrated. This is continuously done by the metrology fringes.

3.4 Design of the payload subsystems

With all these constraints in mind, we have designed the NEAT subsystems which will permit to achieve the main requirements.

Focal plane assembly. A proposition for implementation of the focal plane is shown in Fig. 7. The detector is foreseen to be a CCD fabricated by the E2V technologies company in UK. The target star, the reference star and the telescope axis tracker will all use the same CCD that includes the capability to read windowed images, typically 10×10 to 30×30 pixels. The 8 XY tables consist of two linear tables mounted on top of each other.

Each table uses a piezo-reptation motor*, a linear ball bearing system and an optical incremental encoder. These motors fulfill several requirements of simplicity: they are self-locked when they are not powered; they can be used both for large displacements by stepping up to 100 mm \times 100 mm and elementary analog motion down to 50 nm. Since 8 tables are used in parallel in the focal plane, the loss of one table is not a single point failure. An alternative implementation could be to drive the *XY* tables with ball screws and rotary motors. The limited resolution of such a motor stage (about 5 μ m) could be supplemented by a second high-resolution piezo *XY* table[†], mounted on top of the first *XY* table. The main structure of the focal *XY* tables consists of a large lightweight aluminum cylinder which is thermally controlled and in which pockets are machined for the fixation of the *XY* tables.

Telescope. The primary mirror is an off-axis paraboloid, with a 1 m diameter clear aperture, an off-axis distance of 1 m and a focal length of 40 m. It would be manufactured in either Zerodur or ULE, 70% lightweighted and weight about 60 kg. The surface quality should be better than $\lambda/4$ peak-to-valley and would be coated with protected aluminum. A 50 mm hole at the center of the mirror accommodates the beam launcher for the telescope axis tracker. The three bipods on the back of the mirror support the mirror with minimum deflection. The bipods interface with the tip-tilt stage made of 3 preloaded piezo stacks on parallel flexures that provide the ± 6 arcsecond amplitude for two-axis articulations. The entire primary mirror assembly interface to the telescope payload plate is a 34 kg hogged-out aluminum plate. This plate also hosts the metrology source, the telescope drive electronics, the telescope baffle and the interface to the spacecraft.

Telescope axis tracker. It is used to estimate the location of the primary mirror axis with respect to the focal plane in order to monitor it and then correct for the telescope field dependent errors. The sensor is the second fixed CCD located in the focal-plane. The launcher would consist of either an achromatic doublet or an aspherical singlet lens, embedded in the primary mirror substrate at its center and a single-mode fiber-coupled laser diode.

Laser metrology. The focal-plane metrology system consists of the metrology source similar to the one developed for SIM,⁹ the metrology fiber launchers and the focal plane detectors (CCDs) which alternatively measure the stellar signal (57 s observations) and the metrology (1 s per axis every minute). The metrology fiber launchers consist of nominally four optical fibers attached to the primary mirror substrate. Three of them are located around the edge of the mirror. They are used by pairs in order to conduct three non-redundant measurements of the relative location of the CCDs. The fourth fiber is located inside the clear aperture, and is used in combination with each of the three other fibers to produce three additional measurements during focal plane calibration and calibrate the distance mirror-focal plane.

Pointing servo systems. The pointing of the telescope from one target to the next one is accomplished by the two spacecraft in formation flying. The target stars will be typically separated by 10°. Re-pointing of the telescope will require rotation of the two spacecraft by several degrees using reaction wheels and translation of the telescope spacecraft by several meters using hydrazine propulsion. Fine positioning of the focal plane relative to the mirror is done by cold gas propulsion system. At the end of the maneuver, the telescope spacecraft will be oriented to better than 3 arcseconds from the target star line of sight using star trackers. The focal plane spacecraft will be positioned to better than 2 mm from the primary mirror focus. At that point, the spacecraft will maintain their relative position to better ± 2 mm in shear and in separation for the duration of the observation. The separation does not require a servo-loop of the payload, because its effect is only a degradation in performance (when FWHM increases, final precision decreases in same proportion) and is managed in the error budget.

During the observation, the instrument uses a tip-tilt stage behind the primary mirror to center the target star on the 32 \times 32 pixel sub-window on the target star CCD. Once in the 32 \times 32 pixel sub-frame mode, the target star CCD is read at 500 Hz, and feedback control between the CCD and the tip-tilt stage can be used to keep the star centered on the detector to better than 5 milli-arc-second RMS (0.1 pixel RMS) for the duration of the observation. This is the only active feedback loop in the instrument system working at 50 Hz; the other degrees of freedom (focal plane tip, tilt, clocking and focal-plane-to-mirror separation) are monitored but not corrected

*such reptile motors have been qualified by the Swiss firm RUAG for the LISA GPRM experiment.

[†]such as the Cedrat XY25XS

for in real-time. Prior to acquisition, the reference star CCDs will be pre-positioned to the expected location of the reference stars using the translation stages. The XY translation stage fine motion of the reference star CCDs at a $0.2\ \mu\text{m}$ precision enables centering of the reference stars on the detectors to better than a tenth of a pixel. Once the reference stars are acquired, the translations stages are locked for the duration of the observation.

3.5 Mission requirements

The objectives of the NEAT mission require to perform acquisitions over a large number of targets during the mission timeline, associated to a 40 m focal length telescope satellite. The preliminary assessment of the NEAT mission requirements allows to identify the following main spacecraft design drivers.

Launch configuration and mission orbit. The L2 orbit is the preferred orbit, as it allows best formation flying performance and is particularly smooth in terms of environment. The Soyuz launch, proposed as a reference for medium class missions, offers satisfying performance both in terms of mass and volume.

Formation Flying and 40 m focal length. The mission relies on a 40 m focal length telescope, for which the preferred solution is to use two satellites in formation flying. The performance to be provided by the two satellites in order to initialize the payload metrology systems are of the order of magnitude of $\pm 2\ \text{mm}$ in relative motion, and of 3 arcseconds in relative pointing, which are typically compatible with Formation Flying Units and gyroless AOCS[‡] architecture. At L2, the solar pressure is the main disturbance for formation flying control. As a result, surface-to-mass ratio (S/M ratio) is the main satellite drift contributor and should be as close as possible for the two satellites. Although satellite design can cope with these requirements, the S/M ratio of the satellites will evolve during the mission because of fuel losses and sun angle. However, the preliminary mission assessment tends to demonstrate that the S/M difference between the two satellites can be reduced down to 20-30%, which is deemed compatible with mission formation flying requirements.

Number of acquisitions and Mission ΔV . The mission aims at a complete survey of a large number of targets and the maximization of the number of acquisitions will be a main objective of the next mission phases. The mission objectives require a threshold of 20,000 acquisitions (see Sect. 3.6 for details). In addition, the time allocation for these reconfiguration maneuvers is quite limited, in order to free more than 85% of mission duration for observations. As a result, the mission is characterized by a large ΔV (550 to 880 m/s) dedicated to reconfigurations, plus allocations for fine relative motion initialization and control using the μ -propulsion system. This large number of reconfigurations is also driving the number of thruster firing, which are qualified to typical numbers of up to 5,000 to 50,000 with cycling as required for NEAT.

Baffles and Parasitic Light. The mission performance relies on the ability of the focal plane to receive only star flux reflected by the telescope satellite. A first requirement is to implement baffles on the two satellites, coupled by a diaphragm on the focal plane. In addition, all parasitic light coming from telescope satellite reflections should be avoided, thus requiring all bus elements to be shielded by a black cover.

Following this preliminary satellite requirement analysis, a first simple and robust mission concept has been identified.

3.6 Preliminary Spacecraft Design

The preliminary NEAT mission assessment allowed to identify a safe and robust mission architecture (Fig. 8), relying on high technology-readiness-level (TRL) technologies, and leaving safe margins and mission growth potential that demonstrates the mission feasibility within the medium class mission cost cap.

System Functional Description. The proposed mission architecture relies on the use of two satellites in formation flying. The two satellites are launched in a stacked configuration using a Soyuz ST launcher (Fig. 9), and are deployed after launch in order to individually cruise to their operational Lissajous orbit. Acquisition sequences will alternate with reconfigurations, during which the Telescope Satellite will use its large hydrazine propulsion system to move around the Focal Plane Satellite and to point at any specified star. At the approach of the correct configuration, the Focal Plane Satellite will use a cold gas μ -propulsion system for fine relative motion acquisition. The Focal Plane Satellite will be considered as the chief satellite regarding command and control,

[‡]Attitude and Orbit Control System

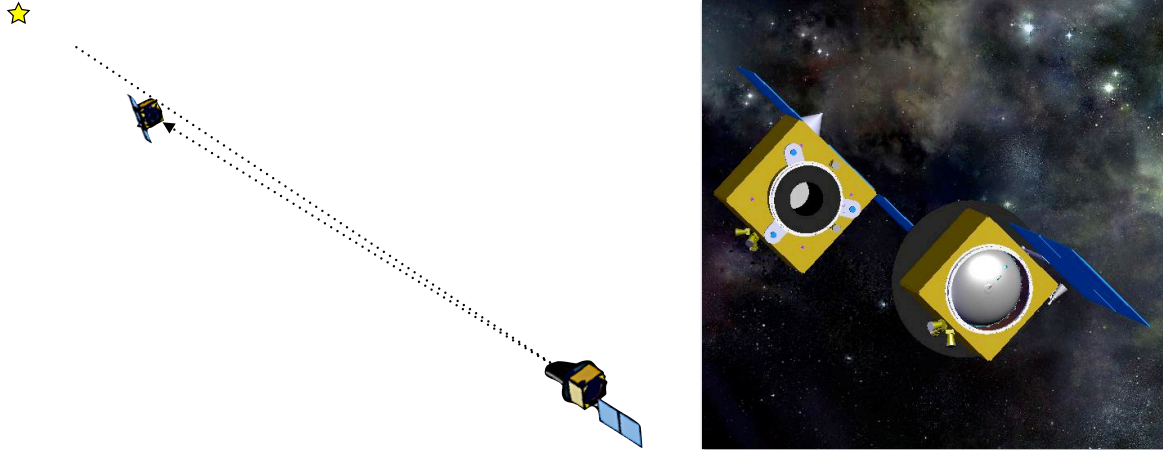


Figure 8. Left: NEAT spacecraft in operation with the two satellites separated by 40 m. Right: closer external view of the two satellites.

communications and payload handling. Communications with the L2 ground station would typically happen on a daily basis through the Focal Plane Satellite, with data relay for TC/TM[§] from the Telescope Satellite using the FFRF[¶] units. This satellite will however be equipped with a similar communication subsystem, in order to support cruise and orbit acquisition, and to provide a secondary backup link.

Formation Flying Architecture. The formation flying will have to ensure anti-collision and safeguarding of the flight configuration, based on the successful PRISMA flight heritage. In addition, the spacecraft will typically perform 12 to 20 daily reconfigurations of less than 10° of the system line of sight corresponding to 7 m of translation of one satellite compared to the other perpendicular to the line of sight. During these configurations, the telescope satellite will perform translations—supported by the FF-RF Units—using its large hydrazine tanks (250 kg) for a $\Delta V \approx 605$ m/s. When the two satellites will approach the required configuration, the telescope satellite will freeze, and the focal plane satellite will perform fine relative pointing control using micro-propulsion system. As a result, the micro-propulsion will have to compensate for hydrazine control inaccuracies, which will require large nitrogen gas tanks (92 kg for $\Delta V \approx 75$ m/s). Finally, 28 kg of hydrazine carried by the FP satellite allows $\Delta V \approx 55$ m/s for station keeping and other operations.

Satellite Design Description. The design of the two satellites is based on a 1194 mm central tube architecture, which will allow a low structural index for the stacked configuration and provides accommodation for payloads and large hydrazine tanks. Strong heritage does exist on the two satellites avionics and AOCS. In addition, they both require similar function which would allow to introduce synergies between the two satellites for design, procurement, assembly, integration and tests. The proposed AOCS configuration is a gyroless architecture relying on reaction wheels and high-performance star trackers (Hydra Sodern), which is compatible with a 3 arcsec pointing accuracy (see end of Sect. 3.4 for payload control). The satellites communication subsystems use X-Band active pointing antenna, supported by large gain antenna for low Earth orbit positioning and cruise, coupled with a 50 W RF Transmitter. The active pointing medium gain antenna allows simultaneous data acquisition and downlink. A reference solution for the satellite on-board computer could rely on the Herschel-Planck avionics.

The two satellites would have custom mechanical-thermal-propulsion architectures. The telescope satellite features a dry mass of 724 kg and the focal plane satellite a dry mass of 656 kg. The focal plane satellite carries the stacked configuration. The payload (focal plane + baffle) are assembled inside a 1194 mm central tube, which will also ensure the stacked configuration structural stiffness. The spacecraft bus, and large cold gas tanks, will be assembled on a structural box carried by the central tube. The proposed architecture uses a large hydrazine tank inside the 1194 mm central tube which offers a capacity of up to 600 kg hydrazine, thus allowing both a

[§]Telecommand / Telemetry

[¶]Formation Flying Radio Frequency

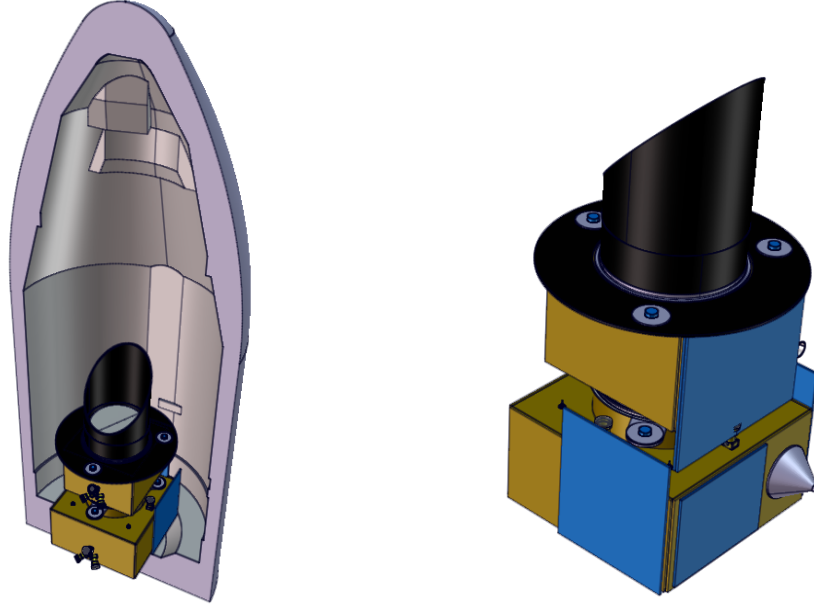


Figure 9. NEAT stowed configuration. Left: in the Soyuz rocket. Right: back view.

low filling ratio and a large mission growth potential. The payload module —with the payload mirror, rotating mechanisms and baffle— is then assembled on the central tube.

Proposed Procurement Approach. The NEAT mission is particularly adapted to offer a modular spacecraft approach, with simple interfaces between payload and spacecraft bus elements. For both satellites, the payload module is clearly identified and assembled inside the structural 1194 mm central tube. In addition, a large number of satellite building blocks can be common to the two satellites, in order to ease mission procurement and tests. This configuration is particularly compatible with the ESA procurement scheme. The payload is made of 3 subsystems: primary mirror and its dynamic support, the focal plane with its detectors and the metrology.

Alternative mission concepts. An alternative mission concept would consist of a single spacecraft with an ADAM-like^{||} deployable boom (from ATK-Able engineering) that connects the telescope and the focal plane modules. The preliminary investigation made by CNES identified no show-stoppers for this option: no prohibitive oscillation modes during observation; during maneuvers, the boom oscillation modes can be excited but they can be filtered by Kalman filters like SRTM demonstrated it. The use of dampers on the boom structure allows damping at a level of 10% of the oscillations. The main worry concerns retargeting, which requires large reaction wheels or control momentum gyroscopes (CMGs) on the spacecraft due to the important inertia but propellers could be added at the boom end. A possible implementation made by JPL is shown in left part of Fig. 10. Concerning a formation flying version, a smaller version of NEAT called μ NEAT (see right part of Fig. 10) has been recently submitted using existing technology (PRISMA and state-of-the-art metrology).

4. DISCUSSION

4.1 Astrophysical issues

Stellar activity. If all instrumental problems are controlled then the next obstacle to achieve the scientific objective is of astrophysical nature, the impact of stellar activity. Spots and bright structures on the stellar surface induce astrometric, photometric and RV signals. Using the Sun as a proxy, Lagrange et al.² have computed the astrometric, photometric and RV variations that would be measured from an observer located 10 pc away. It appears that the astrometric variations due to spots and bright structures are small compared to

^{||}ADAM: ABLE Deployable Articulated Mast

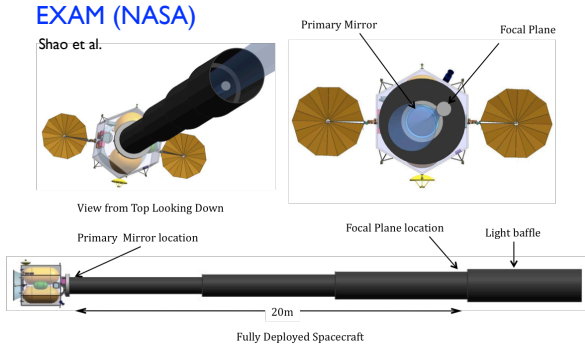


Figure 10. Alternative missions. Left: EXAM, a flight system concept for the deployable telescopic tube version for a 0.6 m version of NEAT. Right: μ NEAT, a formation flying version of NEAT with a 0.3 mirror.

the signal of an Earth mass planet in the HZ.^{10–12} This remains true throughout the entire solar cycle. If we consider a star *5 times more active than the active Sun*, an Earth-mass planet would still be detectable even during the highest activity phases. Such activity, or lower, translates in terms of activity index $\log(R'_{HK}) \leq -4.35$. Consequently, in our target list, we have kept only stars with such an index (*only 4% were discarded*), for which their intrinsic activity should not prevent the detection of an Earth-mass planet, even during its high activity period.

Perturbations from reference stars. The vast majority of the reference stars will be K giants at a distance of ≈ 1 kpc. The important parameters in addition to the position are the proper motion with typical value of ≈ 1 mas/yr and the parallax whose typical value is ≈ 1 mas. They are to be compared to the accuracy of the cumulative measurements during a visit. An important value for NEAT accuracy is what is obtained for an $R = 6$ magnitude target: $0.8 \mu\text{as}/\sqrt{h}$. The ratios between that (required) accuracy and the expected motions of the references indicates clearly that the latter cannot be considered as fixed. Their positions are members of the set of parameters that have to be solved for. Because the reference stars are much more distant (≈ 1 kpc) than the target star (≈ 10 pc), we are 100 times less sensitive to their planetary perturbations. Only Saturn-Jupiter mass objects matter, and statistically, they are only present around $\approx 10\%$ of stars. These massive planets can be searched for by fitting first the reference star system ($\approx 100 N_{\text{ref}}$ measurements for $5 N_{\text{ref}}$ parameters when there are no giant planets around the reference stars), possibly eliminate those with giant planets, and studying the target star with respect to that new reference frame. Moreover, the largest disturbers will be detected from ground based radial velocity measurements, and the early release of Gaia data around 2016 will greatly improve the position accuracy of the reference stars. For smaller planets at or below the threshold of detection, their impact on the target astrometry will be only at a level $\ll 1 M_{\oplus}$ around it. Similarly the activity of these K giants has been investigated and neither the stellar pulsations nor the stellar spots will disturb the signal at the expected accuracy.

Planetary system extraction from astrometric data. We recently carried out a major numerical simulation to test how well a space astrometry mission could detect planets in multi-planet systems.¹³ The simulation engaged 5 teams of theorists who generated model systems, and 5 teams of double-blind “observers” who analyzed the simulated data with noise included. The parameters of the study were the same as for NEAT, viz., astrometric single-measurement uncertainty ($0.80 \mu\text{as}$ noise, $0.05 \mu\text{as}$ floor, 5-year mission, plus RV observations with 1 m/s accuracy for 15 years). We found that terrestrial-mass, habitable-zone planets (\approx Earths) were detected with about the same efficiency whether they were alone in the system or if there were several other giant-mass, long-period planets (\approx Jupiters) present. The reason for this result is that signals with unique frequencies are well separated from each other, with little cross-talk. The number of planets per system ranged from 1 to 11, with a median of 3. The SNR value of 5.8 value was predicted¹⁴ for a false alarm probability (FAP) of less than 1%, and verified in our simulations. The completeness and reliability to detect planets was better than 90% for all planets, where the comparison is with those planets that should have been detected according

Table 3. Science impact of NEAT scaling. The nominal mission is highlighted in yellow.

Mission name	Mirror diameter	Focal length	Field of view diameter	Focal Plane size	Ref. star mean magnitude	DMA in 1h	# targets for a given mass limit		
	(m)	(m)	(deg)	(cm)	(R mag)	(μ as)	$0.5M_{\oplus}$	$1M_{\oplus}$	$5M_{\oplus}$
NEAT plus	1.2	50	0.45	40	11.5	0.7	7	100	200
NEAT	1.0	40	0.56	40	11	0.8	5	70	200
NEAT light	0.8	30	0.71	35	10.5	1.0	4	50	200
EXAM	0.6	20	0.85	30	10.1	1.4	2	35	200
							$1M_{\oplus}$	$10M_{\oplus}$	$50M_{\oplus}$
μ NEAT (*)	0.3	12	0.6	15	11	10.2	2	25	200

DMA = Differential astrometric Measurement Accuracy (mas); (*) centroiding requirement relaxed to 4e-5

to a Cramer-Rao estimate¹⁵ of the mission noise. The Cramer-Rao estimates of uncertainty in the parameters of mass, semi-major axis, inclination, and eccentricity were consistent with the observed estimates of each: 3% for planet mass, $\approx 4^\circ$ for inclination and 0.02 for eccentricity.

Radial velocity screening. To solve unambiguously for giant planets with periods longer than 5 yrs, it is necessary to have a ground RV survey for 15 yrs of the 200 selected target star, at the presently available accuracy of 1 m/s. More than 80% of our targets are already being observed by RV, but the observations of the rest of them should start soon, well before the whole NEAT data is available. The capability of ground based RV surveys, despite their impressive near-term potential to obtain accuracies better than 1 m/s, is not sufficient to detect terrestrial planets in the HZ of F, G and K stars. Formally, an accuracy of 0.05 m/s is required to see an edge-on Earth mass planet at 1 AU from a solar-mass star with $\text{SNR} = 5$, which might be achievable instrumentally, but is stopped in most cases by the impact of stellar activity on RV accuracy. It is necessary to find particularly “quiet” stars, but they are a minority (few percents) and cannot provide a full sample. Furthermore, the ambiguity in physical mass associated with the signal coming only from the radial component of the stellar reflex motion ($\sin i$ ambiguity) requires additional information to determine the physical mass and relative inclination in complex planetary systems. In some, but not all cases, limits are possible, and one can argue statistically that 90% of systems should be oriented such that the physical planet mass is within a factor of two of the mass found in RV. However, for finding a small number of potential future targets for direct detection and spectroscopy, an absolute determination that the mass is Earth-like is required as well as an exhaustive inventory of the planets around stars in our neighborhood.

Flexibility of objectives to upgrades / downgrades of the mission. One of the strengths of NEAT is its flexibility, the possibility to adjust the size of the instrument with impacts on the science that are not prohibitive. The size of the NEAT mission could be reduced (or increased) with a direct impact on the accessible number of targets but not in an abrupt way. For instance, for same amount of integration time and number of maneuvers, the options listed in Table 3 are possible, with impacts on the number of stars that can be investigated down to 0.5 and 1 Earth mass, and on the mass of the instrument, required fuel for maneuvers, and therefore cost. The time necessary to achieve a given precision depends on the mass limit that we want to reach: going from $0.5M_{\oplus}$ to $1M_{\oplus}$ requires twice less precision and therefore 4 times less observing time allowing a smaller telescope. There is room for adjustment keeping in mind that one wants to survey the neighborhood with the smallest mass limit possible and a typical number of targets of ≈ 200 .

4.2 Technical issues

Optical aberrations. NEAT uses a very simple telescope optical design. A 1-m diameter clear aperture off-axis parabola, with an off-axis distance of 1 m and a 40 m focal length. The focal plane is at the prime focus. The telescope is diffraction limited at the center of the field, where the target stars will be observed, but coma produces some field dependent aberrations. At the mean position of the reference stars, 0.2° away from the center of the field, the coma produces a *steady* 23% increase of the point spread function (PSF) width and an $8\ \mu\text{m}$ centroid offset. The impact remains low since we are looking at differential effects.

Centroid measurements. They consist of two steps: the determination of the stellar centroid on each CCD during 57 s and then the calibration of the relative position of the CCDs during 3 s thanks to the metrology. The

metrology determines also the response map of the detectors. As in the normal approach to precision astrometry with CCDs, we perform a least-square fit of a template PSF to the pixelated data. PSF knowledge error leads to systematic errors in the conventional centroid estimation. An accurate centroid estimation algorithm by reconstructing the PSF from well sampled (above Nyquist frequency) pixelated images was developed.^{4,5} In the limit of an ideal focal plane array whose pixels have identical response function (no inter-pixel variation), this method can estimate centroid displacement between two 32x32 images to sub-micropixel accuracy. Inter-pixel response variations exist in real CCDs, which we calibrate by measuring the pixel response of each pixel in Fourier space. Capturing inter-pixel variations of pixel response to the third order terms in the power series expansion, we have shown with simulated data⁴ that the centroid displacement estimation is accurate to a few micro-pixels.

Stability of the primary mirror. The primary optic will be made of zerodur/ULE with a temperature coefficient better than $10^{-8}/\text{K}$ with an optics thickness ≈ 10 cm and the effective temperature and temperature gradients are kept stable to ≈ 0.1 K over the mirror, the optic is then stable to ≈ 0.1 nm ($\lambda/6000$) during the 5 yr mission. We have simulated two images, one at the center of the field that is a perfect Airy function and one at the edge of the field that has a $\lambda/20$ coma. We added also wavefront errors with a conservative rms value of $\lambda/1000$. With the new wavefronts, we calculated the change in the differential astrometry bias caused by both pixelation and changing wavefronts. While the wavefront deviations to optimal shape caused a centroid shift of $\approx 6 - 10 \mu\text{as}$ (10^{-4} pixels), differential errors remained less than $\approx 0.3 \mu\text{as}$ (3×10^{-6} pixels).

CCD damage in L2 environment. CCDs suffer damage in radiation environments**. *Charge Transfer Efficiency* (CTE)^{††}, caused by solar wind protons colliding with the CCD silicon lattice and causing displacement damage, leads to the formation of traps which can capture photo-electrons and release them again after some time. This results in loss of signal and a distortion of the shape of the PSF image, leading to systematic errors in the image location due to a mismatch between the ideal PSF shape and the actual image shape. There are differences between NEAT and Gaia which justify the assumption that radiation damage effects will play a much smaller role: NEAT is looking for extended periods at very bright stars compared to Gaia and is not operated in time-delayed integration mode. The CCDs are also regularly illuminated by the laser light from the metrology system. Therefore the signal level of the pixels is high, which will keep the traps with long release time constants filled and effectively inactive.

CCD/metrology tests in the lab. In the absence of optical errors, the major error sources are associated with the focal plane: (1) motions of the CCD pixels, which have to be monitored to 3×10^{-6} pixels every 60 s, i.e. 0.03 nm; (2) measurements of the centroid of the star images with 5×10^{-6} pixel accuracy. We have set up technology testbeds to demonstrate that we can achieve these objectives. The technology objective for (1) has almost been reached and the technology demonstration for (2) is underway and should be completed soon.^{7,8} Latest results with no metrology nor QE 6-parameter calibration have been obtained from the CCD / metrology test bench with performance better 4×10^{-5} pixel at 100s integration time. The data collected by Nemati et al.⁵ shows that we are only a factor 10 from the final goal and that differential metrology at intervals of minutes is required to reach it.

5. PERSPECTIVES

In the Cosmic Vision plan for 2015-2025, the community has identified in Theme 1 the question: “*What are the conditions for planet formation?*”, and the recommendation in Sect. 1.2: “*Search for planets around stars other than the Sun...*” ultra high precise astrometry as a key technique to explore our solar-like neighbors.

“On a longer timescale, a complete census of all Earth-sized planets within 100 pc of the Sun would be highly desirable. Building on Gaia’s expected contribution on larger planets, this could be achieved with a high-precision terrestrial planet astrometric surveyor.”

**<http://www.rssd.esa.int/gaia>

††The Gaia community speaks of the complementary quantity, charge transfer inefficiency (CTI), in order to emphasize its detrimental effects.

We have designed NEAT to be this astrometric surveyor. In Europe, as discussed in detail in the conclusions of the conference *Pathways to Habitable Planets*¹⁶ and in the *Blue Dot Team* report, the exoplanet community recognizes the importance of astrometric searches for terrestrial planets and has prioritized this search as a key question in the mid-term, i.e. in the time frame 2015-2022. The ExoPlanet Task Force (ExoPTF) in the US made a similar statement. Finally the ESA dedicated *ExoPlanetary Roadmap Advisory Team* (EPRAT) prioritizes *Astrometric Searches for Terrestrial Planets* in the mid term, i.e. in the time frame 2015-2022. Although the Decadal Survey of Astronomy and Astrophysics for 2010-2020 ranked down the SIM-Lite proposal, but placed as number one priority a program “to lay the technical and scientific foundation for a future mission to study nearby Earth-like planets”.

Because of these recommendations by the community, we believe that there is a place for a mission like NEAT in future space programs, that is to say, a mission that is capable of detecting and characterizing planetary systems orbiting bright stars in the solar neighborhood that have a planetary architecture like that of our Solar System or an alternative planetary system partly composed of Earth-mass planets. These stars visible with the naked eye or simple binoculars, if found to host Earth-mass planets, will change humanity’s view of the night sky.

ACKNOWLEDGMENTS

This work has benefited support from the Centre National des Études Spatiales (CNES), the Jet Propulsion Laboratory (JPL), Thales Alenia Space (TAS), Swedish Space Corporation (SSC) and the Labex OSUG@2020. AC PhD fellowship is funded by CNES and TAS.

REFERENCES

- [1] van Leeuwen, F., “Validation of the new Hipparcos reduction,” *A&A* **474**, 653–664 (Nov. 2007).
- [2] Lagrange, A., Meunier, N., Desort, M., and Malbet, F., “Using the Sun to estimate Earth-like planets detection capabilities . III. Impact of spots and plages on astrometric detection,” *A&A* **528**, L9+ (Apr. 2011).
- [3] Kaltenecker, L., Eiroa, C., Ribas, I., Paresce, F., Leitzinger, M., Odert, P., Hanslmeier, A., Fridlund, M., Lammer, H., Beichman, C., Danchi, W., Henning, T., Herbst, T., Léger, A., Liseau, R., Lunine, J., Penny, A., Quirrenbach, A., Röttgering, H., Selsis, F., Schneider, J., Stam, D., Tinetti, G., and White, G. J., “Stellar Aspects of Habitability - Characterizing Target Stars for Terrestrial Planet-Finding Missions,” *Astrobiology* **10**, 103–112 (Jan. 2010).
- [4] Zhai, C., Shao, M., Goullioud, R., and Nemati, B., “Micro-pixel accuracy centroid displacement estimation and detector calibration,” *Royal Society of London Proceedings Series A* **467**, 3550–3569 (Dec. 2011).
- [5] Nemati, B., Shao, M., Zhai, C., Erlich, H., Goullioud, R., and Wang, X., “Micropixel-level image position sensing testbed,” in [*Society of Photo-Optical Instrumentation Engineers (SPIE) Conference Series*], *Society of Photo-Optical Instrumentation Engineers (SPIE) Conference Series* **8151** (Sept. 2011).
- [6] Guyon, O., Shaklan, S., Levine, M., Cahoy, K., Tenerelli, D., Belikov, R., and Kern, B., “The pupil mapping exoplanet coronagraphic observer (PECO),” in [*Society of Photo-Optical Instrumentation Engineers (SPIE) Conference Series*], *Presented at the Society of Photo-Optical Instrumentation Engineers (SPIE) Conference* **7731** (July 2010).
- [7] Nemati, B., Shao, M., Zhai, C., and Goullioud, R., “Progress towards precision focal-plane astrometry using micropixel centroiding,” in [*Society of Photo-Optical Instrumentation Engineers (SPIE) Conference Series*], *Society of Photo-Optical Instrumentation Engineers (SPIE) Conference Series* **8442** (Sept. 2012).
- [8] Crouzier, A., Malbet, F., Preis, O., Henault, F., Kern, P., Guillermo, M., Feautrier, P., Cara, C., Lagage, P., Léger, A., Le Duigou, J., Shao, M., and Goullioud, R., “An experimental testbed for NEAT to demonstrate micro-pixel accuracy,” in [*Society of Photo-Optical Instrumentation Engineers (SPIE) Conference Series*], *Society of Photo-Optical Instrumentation Engineers (SPIE) Conference Series* **8442** (Sept. 2012).
- [9] Erlich, H., Qiu, Y., Poberezhskiy, I., Meras, P., and Wu, J., “Reliable optical pump architecture for highly coherent lasers used in space metrology applications,” *SPIE* **7734** (July 2010).
- [10] Meunier, N., Lagrange, A., and Desort, M., “Reconstructing the solar integrated radial velocity using MDI/SOHO,” *A&A* **519**, A66+ (Sept. 2010).

- [11] Makarov, V. V., Beichman, C. A., Catanzarite, J. H., Fischer, D. A., Lebreton, J., Malbet, F., and Shao, M., “Starspot Jitter in Photometry, Astrometry, and Radial Velocity Measurements,” *ApJ* **707**, L73–L76 (Dec. 2009).
- [12] Makarov, V. V., Parker, D., and Ulrich, R. K., “Astrometric Jitter of the Sun as a Star,” *ApJ* **717**, 1202–1205 (July 2010).
- [13] Traub, W. A., Beichman, C., Boden, A. F., Boss, A. P., Casertano, S., Catanzarite, J., Fischer, D., Ford, E. B., Gould, A., Halverson, S., Howard, A., Ida, S., Kasdin, N. J., Laughlin, G. P., Levison, H. F., Lin, D., Makarov, V., Marr, J., Muterspaugh, M., Raymond, S. N., Savransky, D., Shao, M., Sozzetti, A., and Zhai, C., “Detectability of Earth-like Planets in Multi-Planet Systems: Preliminary Report,” *EAS Pub. Series* **42**, 191 (2010).
- [14] Scargle, J. D., “Studies in astronomical time series analysis. II - Statistical aspects of spectral analysis of unevenly spaced data,” *ApJ* **263**, 835–853 (Dec. 1982).
- [15] Gould, A., Dong, S., Gaudi, B. S., Udalski, A., Bond, I. A., Greenhill, J., Street, R. A., Dominik, M. e. a., and MiNDSTEp Consortium, “Frequency of Solar-like Systems and of Ice and Gas Giants Beyond the Snow Line from High-magnification Microlensing Events in 2005-2008,” *ApJ* **720**, 1073–1089 (Sept. 2010).
- [16] Coudé Du Foresto, V., Gelino, D. M., and Ribas, I., “Pathways Towards Habitable Planets,” *ASPC Series* **430** (Oct. 2010).